



**HAL**  
open science

## The thermospheric auroral red line Angle of Linear Polarization

Jean Lilensten, Mathieu Barthélemy, Gérard Besson, Hervé Lamy, Magnar G. Johnsen, Jøran Moen

► **To cite this version:**

Jean Lilensten, Mathieu Barthélemy, Gérard Besson, Hervé Lamy, Magnar G. Johnsen, et al.. The thermospheric auroral red line Angle of Linear Polarization. *Journal of Geophysical Research Space Physics*, 2016, 121, pp.7125-7134. 10.1002/2016JA022941 . insu-03634248

**HAL Id: insu-03634248**

**<https://insu.hal.science/insu-03634248>**

Submitted on 7 Apr 2022

**HAL** is a multi-disciplinary open access archive for the deposit and dissemination of scientific research documents, whether they are published or not. The documents may come from teaching and research institutions in France or abroad, or from public or private research centers.

L'archive ouverte pluridisciplinaire **HAL**, est destinée au dépôt et à la diffusion de documents scientifiques de niveau recherche, publiés ou non, émanant des établissements d'enseignement et de recherche français ou étrangers, des laboratoires publics ou privés.

Copyright

## RESEARCH ARTICLE

10.1002/2016JA022941

## The thermospheric auroral red line Angle of Linear Polarization

Jean Lilensten<sup>1</sup>, Mathieu Barthélemy<sup>1</sup>, Gérard Besson<sup>2</sup>, Hervé Lamy<sup>3</sup>, Magnar G. Johnsen<sup>4</sup>, and Jøran Moen<sup>5</sup>

## Key Points:

- First calibrated measurement of the auroral red line Angle of Linear Polarization (AoLP)
- The AoLP is a tracer of the magnetic field configuration
- It has impacts in space weather and planetary researches

## Supporting Information:

- Supporting Information S1

## Correspondence to:

J. Lilensten,  
jean.lilensten@univ-grenoble-alpes.fr

## Citation:

Lilensten, J., M. Barthélemy, G. Besson, H. Lamy, M. G. Johnsen, and J. Moen (2016), The thermospheric auroral red line Angle of Linear Polarization, *J. Geophys. Res. Space Physics*, *121*, 7125–7134, doi:10.1002/2016JA022941.

Received 12 MAY 2016

Accepted 6 JUL 2016

Accepted article online 12 JUL 2016

Published online 23 JUL 2016

<sup>1</sup>Institut de Planétologie et d'Astrophysique de Grenoble, UGA/CNRS-INSU, Grenoble, France, <sup>2</sup>Institut Fourier, Université de Grenoble, Grenoble, France, <sup>3</sup>Belgian Institute for Space Aeronomy, Brussels, Belgium, <sup>4</sup>Tromsø Geophysical Observatory University of Tromsø, Tromsø, Norway, <sup>5</sup>Department of Physics, University of Oslo, Oslo, Norway

**Abstract** The auroral red line at 630 nm is linearly polarized. Up to now, only its Degree of Linear Polarization had been studied. In this article, we examine for the first time the Angle of Linear Polarization (AoLP) and we compare the measurements to the apparent angle of the magnetic field at the location of the red line emission. We show that the AoLP is a tracer of the magnetic field configuration. This opens new perspectives, both in the frame of space weather and in the field of planetology.

## 1. Introduction

The red line is a triplet at 630.0, 636.4, and 639.2 nm and is one of the most intense lines in the auroral spectrum. It originates in the deactivation of the metastable O(<sup>1</sup>D) state. The polarization of the thermospheric atomic oxygen red line at 630 nm was discovered in Lilensten *et al.* [2008] with a dedicated photopolarimeter (hereafter called SPP) described in the above mentioned article. In Lilensten *et al.* [2006], we suggested that the Angle of Linear Polarization (AoLP) of this line could be a tracer of the magnetic configuration. Indeed, the precipitating electrons enter the upper atmosphere with their center of mass following the magnetic field line. Secondary electrons, although less focused [Porter *et al.*, 1987; Lilensten *et al.*, 2015], still follow the magnetic field lines. The oxygen atoms are then mostly hit by primary and secondary electrons with a well-focused pitch angle, and it is likely that the emission due to the deexcitation vibrates globally in a homogenous direction. In Bommier *et al.* [2011] it was shown theoretically that the AoLP should be parallel to the local magnetic field. This paper aims at checking this prediction using data obtained during a 2015 campaign in Ny-Ålesund.

## 2. The 2015 Ny-Ålesund Campaign

## 2.1. Observational Conditions

The SPP consists mostly of two photo multipliers (PMs). An interference filter centered on the 630 nm red line (with a band pass of 1 nm) is located in front of each PM. A polarizing filter is rotating in front of one PM. We call it the “polarized channel,” while the PM without polarizer is referred to as the “reference channel.” The field of view is 2°. There are 80 measurements per full rotation of the polarizing filter, so that the experimental resolution for the AoLP is  $\pm 2.25^\circ$ . The uncertainty on the AoLP will depend on the S/N ratio of individual measurements since the AoLP (and Degree of Linear Polarisation (DoLP)) is determined by fitting a  $\cos^2$  curve to the raw data [Lilensten *et al.*, 2013].

The SPP was installed in the research station of Ny-Ålesund (78.62° geographic north latitude, 11.63° geographic longitude), in the Svalbard archipelago in October 2014. The permanent staff from Alfred Wegener Institute and the French Polar Institute Paul Emile Victor Arctic Research Base was trained to operate it during the winter. A list of favorable times for observation was prepared, when both the Sun and the Moon were at least 18° below the horizon. The weather is, of course, another strong limitation. In Lilensten *et al.* [2015], it was shown by comparing the polarization modeling with data from the SPP and from the incoherent scatter radar European Incoherent Scatter (EISCAT), which the red line polarization maximizes around 220 km. This altitude may depend on the geomagnetic activity because the thermospheric composition itself varies with the geomagnetic activity and introduces some uncertainties in the comparison between measurements and the theory, as will be discussed below. In the following, we call H the point where the line of sight of SPP crosses the altitude  $h = 220$  km. The SPP was pointing with an elevation of 30° toward magnetic west during the whole winter. With an azimuth reference of 0° for geographic north and 90° toward geographic east, magnetic west has an azimuth of 279°. With these parameters, the theoretical apparent angle of the magnetic field at H as

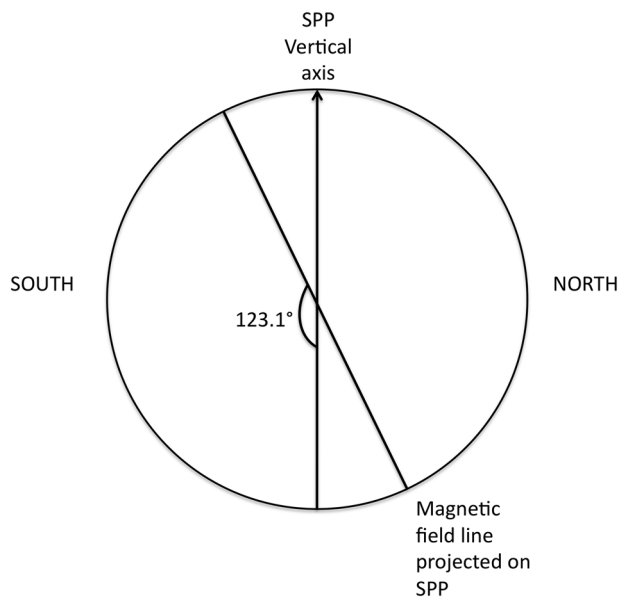


**Figure 1.** The circle represents the aperture of the polarized channel in the SPP. In this example, the apparent angle of the magnetic field on the SPP (123.1°) is that of the magnetic west pointing with an elevation of 30°.

seen by the SPP is  $123.10 \pm 0.2^\circ$ . (The computation of this angle is a classical spherical geometry problem whose detail is provided in the supporting information.) The error is simply when taking into account that the red line is actually emitted between about 180 km where this angle is  $123.08^\circ$  and about 300 km where this angle is  $123.12^\circ$ . To make clear what this angle means, the geometry is shown in Figure 1.

The winter campaign was organized in two phases. In the first part, the SPP was pointing continuously in the direction indicated above while, in February 2015, a dedicated campaign was organized in order to point in different magnetic directions. However, on 23 December, a failure occurred in the instrument with the rotation of the lens becoming irregular, preventing us from exploiting the data after this date, in spite of many efforts to retrieve them. Therefore, only a few hours are available from the whole period. The summary of the winter campaign is given in Table 1.

**2.2. Data Processing and Calibration of SPP**

The processing of SPP data has been gradually improved over the years to obtain the calibrated DoLP. In *Lilensten et al.* [2008], a simple Fourier transform was used. The process was later improved in *Lilensten et al.* [2013] to take account of the instrumental polarization using the Mueller formalism [*Goldstein, 2003; Stenflo, 1994; Martinez Herrero et al., 2009; Clarke, 2010*]. Recently, this latter approach was again improved by taking

**Table 1.** Observation Times<sup>a</sup>

Start (Day)	Start (UT)	End (Day)	End (UT)
20 Oct	20.00	20 Oct	21.78
29 Oct	18.75	30 Oct	0.97
30 Oct	18.58	30 Oct	20.56
19 Nov	16.75	20 Nov	5.25
29 Nov	23.25	30 Nov	6.00
19 Dec	15.50	20 Dec	7.00
20 Dec	15.50	21 Dec	7.00
21 Dec	15.50	22 Dec	7.00

<sup>a</sup>The starting and closing UT are in decimal hours. North direction is on the right and south on the left.

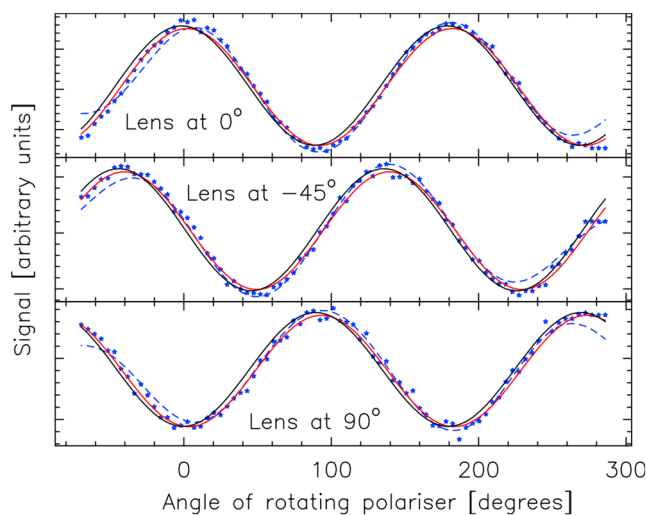


**Figure 2.** Calibration of the observed Angle of Linear Polarization. The stars represent the raw measurements obtained in an optical laboratory with a calibrating polarizing lens. The dashed blue line is the measurements low pass filtered. The red line is the signal reconstructed from a  $\cos^2$  fit on the filtered data as in *Lilensten et al.* [2008]. The black line is the signal reconstructed from the Stokes parameters deduced with a time-dependent Mueller method as in *Lilensten et al.* [2015]. (top) The polarization lens orientation (with respect to the vertical axis) was  $0^\circ$ . (middle) The polarization lens was at  $-45^\circ$ . (bottom) The polarization lens was at  $90^\circ$ , i.e., horizontal.

into account the temporal variability of the polarization during the rotation of the polarizing lens [*Lilensten et al.*, 2015]. All three data processing are still used and are compared in Figure 2 on a set of calibration tests where an additional polarization lens was placed in front of the polarized channel and oriented along different angles with respect to the vertical axis. In the figure, we show the results for three angles of  $0^\circ$ ,  $-45^\circ$ , and  $90^\circ$ . The three methods give very similar results, but for field measurements (where the polarization and intensity of the red line emission can change quickly), the time-dependent Mueller formalism is much more rigorous. In the following, we only provide the results obtained using this data processing, although we carefully checked that the other processings give close estimates. In Figure 3, we show an example of what the data and the signal processing looks like.

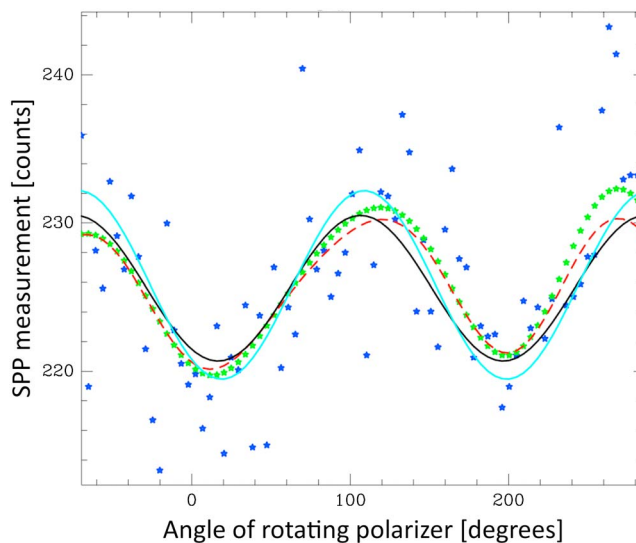


**Figure 3.** Example of a dump analysis, taken on 20 October 2014 at 21 UT. The blue stars are the raw measurements. The green stars show the raw data after high-pass filtering, while the red dashed line is after filtering and averaging over seven points. The black continuous line is the first polarization estimate from the filtered data. The blue continuous line is the polarization from the time-dependent Mueller processing.

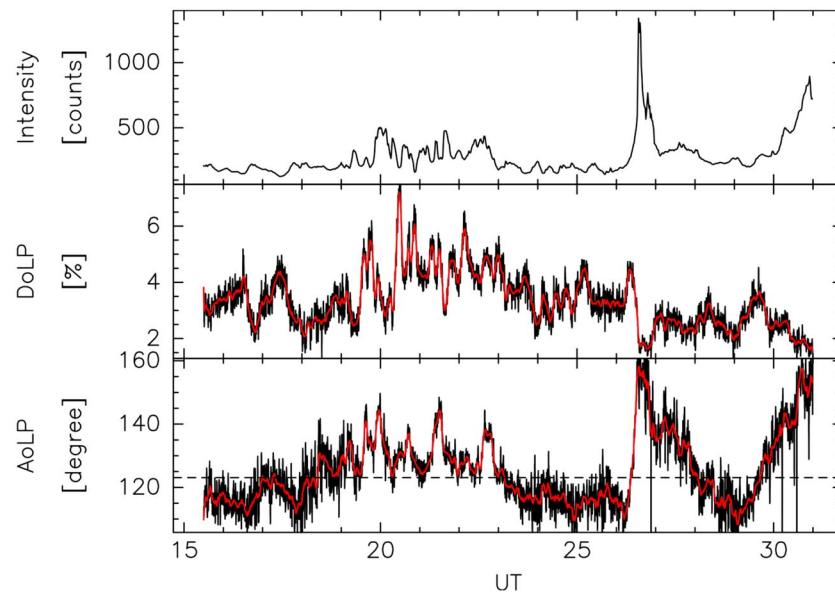


**Figure 4.** The SPP measurement on 21 December 2014. (top) The intensity of light measured by the SPP. (middle) The DoLP and (bottom) The AoLP. The black lines are the 4 s calculation. The red line is the average to compare with the magnetic data. The dashed horizontal line is the theoretical computed value of 123.10°.

**2.3. The SPP Measurements**

During the full winter, we could extract eight periods with continuous measurements. They are summarized in Table 1. Figure 4 shows one example of observations on 21 December 2014. From Figure 4 (top to bottom) are shown respectively the total intensity as measured in the reference channel, the DoLP, the AoLP, the local magnetic field inclination, and declination at the Ny-Ålesund magnetometer. Most of the time the intensity is only slightly larger than 200 counts, which is a very low number corresponding to a very faint auroral activity well reflected in the quite homogeneous magnetometer data. A series of small and short enhancements is observed around 20–22 UT, as well as a larger increase (~1000 counts) around 27 UT (corresponding to 3 UT of next day) and a slower but constant enhancement at the end of the night. Unfortunately, the geomagnetic activity remained quiet all over the wintering.

As already seen in the previous articles, the DoLP follows more or less inversely the intensity of the red line. This is obvious for example for the two intensity peaks just before 27 UT. However, as noted in previous articles, although this trend seems to be a common feature, it is not systematic. For example, the DoLP exhibits a decrease at about 28:5 UT which does not correspond to a noticeable increase in the intensity.

The AoLP also experiences variations (which correspond to a series of rotations, see Figure 1) that can be compared to the intensity variations. The most spectacular variations are observed between 26 UT and 27 UT. When all the points (68,149 points) are taken into account, the mean AoLP is equal to 125.76°, and the mean DoLP corrected from the angle between the line of sight and the magnetic field line in H (equation (22) in the supporting information) is equal to 2.66%. If we take into account, only the quiet periods with no significant

**Table 2.** Geographic Latitudes and Longitudes of the Magnetograms and Keograms Used in This Study

	Latitude (deg)	Longitude (deg)
Ny-Ålesund	78.92	11.93
Danmarkhavn	76.77	-16.66
Bjørnøya	74.5	19.00
Tromsø	69.66	18.94
Skibotn	69.35	20.36

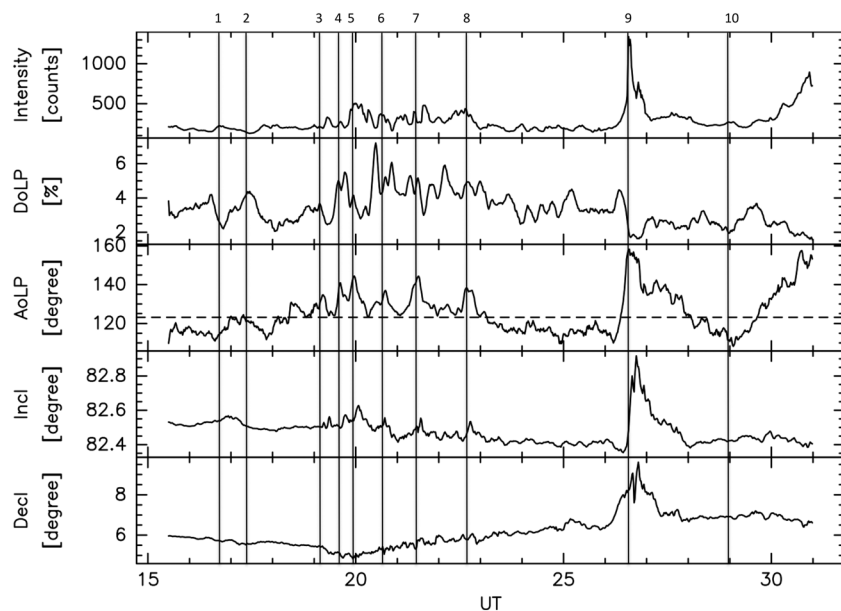


**Figure 5.** (first panel) The intensity of light measured by the SPP, 21 to 22 December 2014. (second panel) The 1 mn averaged DoLP. (third panel) The 1 mn averaged AoLP. The dashed horizontal line is the theoretical computed value of 123.10°. The (fourth panel) inclination and (fifth panel) declination measured by the Ny-Ålesund magnetometer in (°).

increase of the intensity (intensity smaller than 260 counts), the average (on 53,829 points) is exactly equal to the expected theoretical value of 123.10° (see section 2.1). During these quiet periods only, the mean DoLP is equal to 2.79%, a slightly higher value, as expected from previous studies.

The same behavior was observed during the eight periods of measurements. In the following figures, the DoLP only reaches 6% in rare occasions. The AoLP varies globally between 100 and 140 with some excursions at higher values (i.e., closer to the vertical). This will now be discussed in detail.

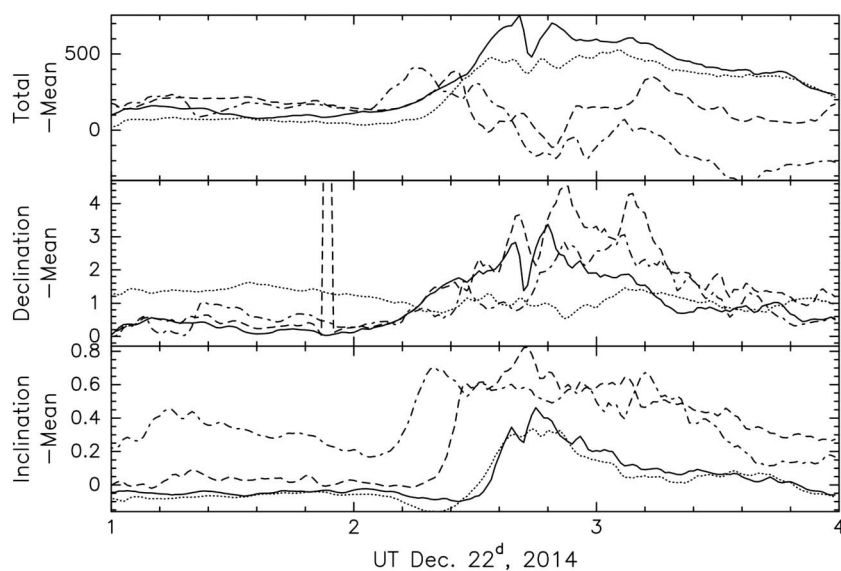


**Figure 6.** Comparison between the magnetograms at Ny-Ålesund (continuous lines), Danmarkhavn (dotted lines), Bjørnøya (dashed lines) and Tromsø (dash-dotted lines), 22 December corresponding to the event 9 in Figure 5. The means are given in Table 3. (top) Total intensity of the magnetic field (nT). (middle) Declination (degrees). (bottom) Inclination (degrees).

**Table 3.** Means Values for the Total Magnetic Field, the Inclination, and the Declination Used in Figure 6

	Total (nT)	Declination (deg)	Inclination (deg)
Ny-Ålesund	54744	6.24	82.45
Danmarkshavn	54391	5.34	81.88
Bjørnøya	54272	0.03	80.67
Tromsø	53484	6.02	78.24

### 3. Comparison Between Measured Polarization and the Local Magnetic Field Configuration

In this section we aim at comparing the polarization data to quantities describing the geomagnetic activity given by local magnetometers. Two magnetometers are roughly at the same distance to the point H. One is located in Danmarkshavn (see the geographic coordinates in Table 2), and comparisons to these data are done in section 3.2. The other one is located in Ny-Ålesund, a few meters away from the SPP and is used in the other sections. The distance between Ny-Ålesund and the intersection with the ground of the line between center of Earth and point H is 420 km, so that this analysis must still be considered with care (see also the discussion in

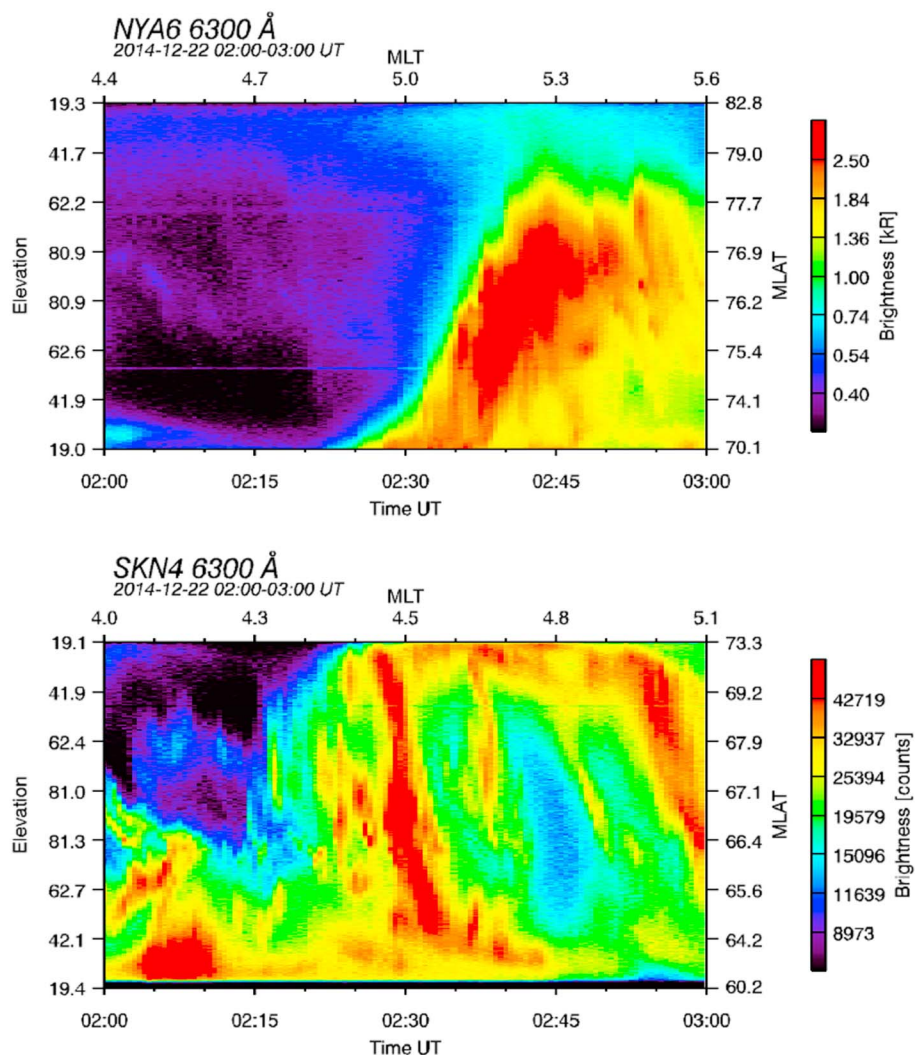


**Figure 7.** Keograms at (top) Ny-Ålesund and (bottom) Skibotn, 22 December corresponding to the event 9 in Figure 5.

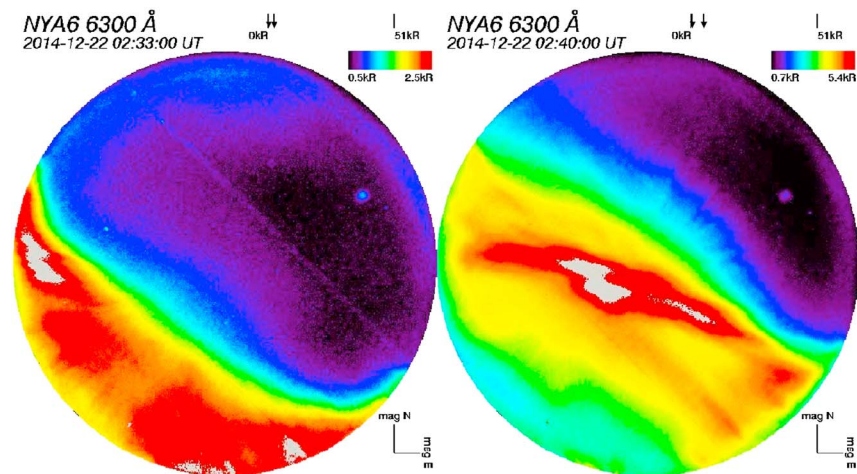


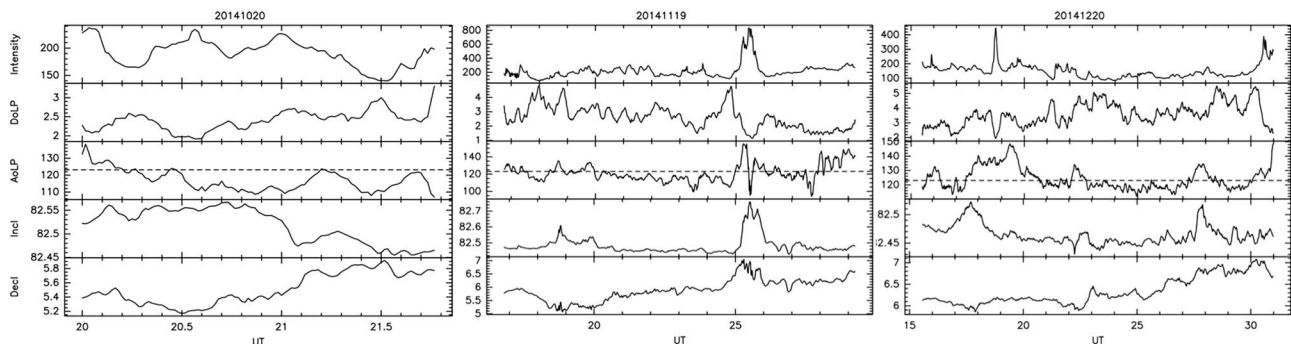
**Figure 8.** All-sky cameras at Ny-Ålesund ((left) 2.33 UT and (right) 2.40 UT), 22 December corresponding to the event 9 in Figure 5.

section 4). Indeed, a variation of the red line intensity will modify the measured polarization instantaneously, while the moment when the magnetometer will experience a modification may be delayed by a few minutes if the same feature moves, e.g., above Ny-Ålesund.

The magnetometer gives a value every minute (higher rates — 10 s — are available but bring no new insight in the frame of the current study). In order to make a direct comparison, the AoLP and DoLP were averaged with a 1 mn sliding window. The resulted values are shown in red in Figure 4.

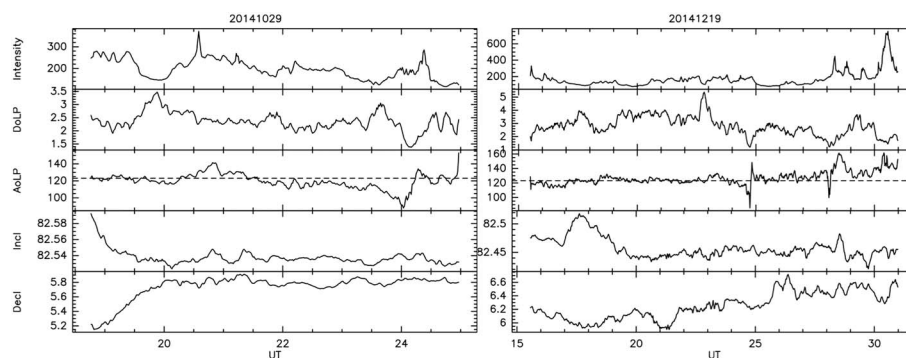
### 3.1. Detailed Study of Data From 21 December 2014

Figure 5 is similar to Figure 4, but only the 1 min average data of DoLP and AoLP are plotted in order to facilitate the comparison with the magnetometer data, shown in the fourth and fifth panels. In this figure, we consider 10 specific instants shown as vertical lines which are numbered 1 to 10. Instant 1 corresponds to a slight increase in the intensity, but a large decrease in the DoLP. The AoLP hardly exhibits any salient feature. Between instants 1 and 2, the inclination has a small enhancement which seems to be visible also in the AoLP. The series of enhancements around instants 3, 4, and 5 are seen a few minutes later in the magnetometer data. The decrease in the intensity shortly before instant 6 is reflected as an increase in the DoLP but has no visible counterpart in the AoLP nor in the magnetometer data. The following increase in the intensity (instant 6) is seen as a decrease in the DoLP, and as an increase of the AoLP, and seen also on the inclination of the magnetic field. Instants 7 and 8 exhibit the same features. This is more spectacular at instant 9, which corresponds to the only strong event during that period of observation. Here the intensity increases up to about 1300 counts, which corresponds to an aurora visible to the naked eye. The decrease in the DoLP is large, about 2%. The AoLP projected on the SPP turns drastically from 118° to 148°. This auroral event is large scale and occurs simultaneously above Ny-Ålesund, as can be seen in the magnetometer data, for both the inclination and the declination. It is interesting to note that the intensity decreases sharply, while the AoLP decreases with a



**Figure 9.** Comparison between the SPP measurements and the magnetometer for (left) 20 October, (middle) 19 November, and (right) 20 December.





**Figure 10.** Comparison between the SPP measurements and the magnetometer for (left) 29 October and (right) 19 December.

slower rate, similar to the variations observed with the magnetometer. After instant 10, the intensity starts to increase again, with an immediate corresponding slow decrease of the DoLP but a large increase of the AoLP. This event is local (near point H) since it is not seen in the magnetometer data.

### 3.2. Enlarging the View: From Local Comparison to Large-Scale Comparison

As stated above, the goal of this article is to show what kind of information the AoLP might provide. In this aim, the best comparison is with data from local magnetometers. Considering a larger picture, i.e., the link to regional or even global geomagnetic activity, is out of the scope of this article. It will be done in future studies when more data covering a larger span of the solar cycle and various solar activity cases will be collected. This paragraph is a first attempt in this direction, aiming to show what could be expected from such a comparison. We shall arbitrarily focus on event 9 during the 21 December 2014 experiment where a clear consistency between the polarization and the magnetometer measurements is observed. This consistency is still observed when we use data from the magnetometer in Danmarkshavn, located approximately on the same magnetic latitude. The data from both ground-based magnetometers (Figure 6) confirm that we are looking at a large-scale current system. This is further confirmed by looking at the University of Oslo keograms from Ny-Ålesund and Skibotn shown in Figure 7: a classic substorm expanding in a large range of latitudes is clearly visible as is confirmed by the aurora moving northward.

Since this event occurs so long after magnetic midnight and is seen also at Danmarkshavn, it is clear that we are located in the morning ionospheric convection cell and that we have a substorm electrojet flowing across the Barents sea and up toward northern Greenland (negative bay indicates a westward flowing current). Looking at the all-sky camera images from the same day at 2.33 and 2.40 UT (Figure 8), we also see that the aurora covers a large portion of the sky all the way to the zenith in Ny-Ålesund. It is therefore safe to assume that we are looking at a current system that covers both the point H, Danmarkshavn, and Ny-Ålesund (i.e., large area in longitude and latitude) and that H lies within the area of precipitation. In other words, it is the large-scale magnetospheric-ionospheric current system that is responsible for the variations in AoLP observed in this study case.

### 3.3. Additional Observations

In Figure 9, data of three other nights are shown where the AoLP and the DoLP are sometimes well correlated with the magnetometer data, and sometimes not. On 20 October (Figure 9, left), a rotation of the AoLP at about 21.3 UT is reflected in the inclination. On 19 November (Figure 9, middle), the only auroral event between 25 and 26 UT (1 to 2 UT on 20 November) is seen also by the magnetometer, with the usual decrease of the DoLP and the rotation of the AoLP. On 20 December (Figure 9, right), an enhancement of the inclination at 28 UT (4 UT on 21 December) corresponds to a rotation of the AoLP from 116 to 130°. In Figure 10, the intensity reaches even smaller values than during the other nights, and the magnetic field inclination is remarkably constant over a large period of time. Then, the measured AoLP is almost exactly the theoretical value of 123.10°.

## 4. Discussion and Conclusion

Ny-Ålesund is located inside the auroral oval, in the polar cap, where low-energy electrons from the polar rain are permanently precipitating [see, e.g., Schunk and Nagy, 2004]. The center of mass of a precipitating

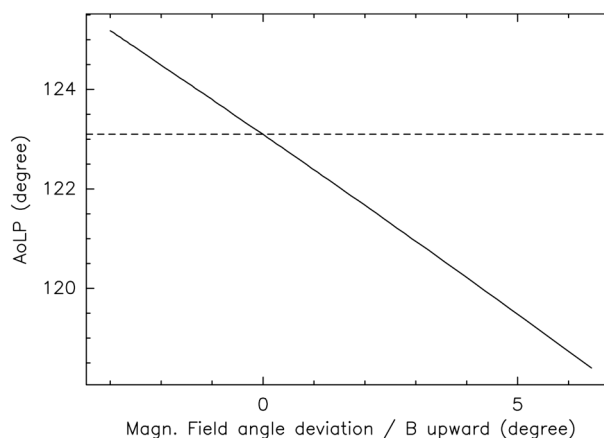


**Figure 11.** Variability of the AoLP for a variation of the angle between the magnetic field in H and its upward component. The dashed line is the theoretical  $123.10^\circ$  value.

electron follows the magnetic field line, while the electron itself rotates around the line. Following the Biot and Savart law, this rotation produces a magnetic field which is superimposed upon the geomagnetic field. This perturbation evolves in time and depends on the energy and particle fluxes of the precipitating electrons. It exists even when the energy of the electrons is small.

The red line emission is due to electrons hitting the oxygen atoms. Since the polar rain is persistent, there is always some red line emission above Ny-Ålesund. For SPP, this background emission due to primary electrons with initial energies below typically 500 eV [Lilensten *et al.*, 2015] results in a measurement of the intensity of  $\sim 100$ –300 counts. On one hand, even with such low energies, there may still be a magnetic perturbation if the electrons are distributed homogeneously (i.e., with similar pitch angles and gyroradii) although there may be no measurable variation in the red line intensity. This is observed several times in the measurements presented in this paper. On the other hand, in order to get a measurable value of the polarization of the red line, the oxygen atoms must also be hit by electrons with homogeneous pitch angles/gyroradii. If the electrons pitch angles are more equally distributed, the directions of the polarization angles would be more distributed as well (see the study of the parameters in Lilensten *et al.* [2015]).

The precipitating electrons have therefore two effects: (1) they influence the local auroral emissions (including the polarization) and (2) they slightly modify the local magnetic field. In the previous section, it was shown that the AoLP measurements may reflect both changes but not systematically. Sometimes, it may reflect accurately the modification of the local magnetic field. However, the AoLP variation cannot be immediately converted into a variation of the local magnetic field. In order to illustrate it, we studied the variation of the AoLP when the angle between the magnetic field in H and its upward component varies. This is shown in Figure 11. In this study, the absolute value of the magnetic field in H (50,100 nT from International Geomagnetic Reference Field, IGRF [Olsen *et al.*, 2000]) is assumed to be constant. We see that a variation of the AoLP between  $118$  and  $125^\circ$  corresponds to a variation of the angle between the magnetic field and its upward component between  $-3$  and  $6.5^\circ$ , respectively. It corresponds to a variation of the upward component between 50,094 and 49,294 nT, i.e., a variation of 1.6% but also to an unlikely variation of the northward component between 6360 and 8946 nT, i.e., a variation of 40%, which can hardly be trusted. This proves that the variability of the AoLP depends not only on the magnetic field orientation but also strongly on the pitch angle distribution of the precipitating electrons on the oxygen atoms as was foreseen in Bommier *et al.* [2011].

Another consideration must be taken into account: the influence of the horizontal currents flowing in the E layer at 110 km. If we assume the point H to be at 220 km, it is roughly located at the same distance from these currents than we are when we measure on the ground. Therefore, we could assume that the measurements in H should be very similar to what we measure on the ground and that the same currents are creating the variable magnetic field which is superimposed on the Earth's internal field. But there are a few exceptions:

1. On the ground we will see a larger contribution from the crustal field, simply since we are closer to the source.

2. On the ground we will see a larger contribution from induced currents in the crust (induced by the variations in the field created by the ionospheric currents).
3. On the other hand, in H, we will see a contribution from field-aligned currents that are not easily apparent in ground-based measurements [Fukushima and Kamide, 1973].

It is difficult to proceed much further in this discussion. On a physical point of view, the differences might be attributed to the points mentioned above. But we also have intrinsic limitations due to the experimental conditions. The first limitation is the aperture of the polarimeter. The field of view ( $2^\circ$ ) is not uniformly illuminated at times when there are discrete structures in the aurora. Auroral arcs are well known to be possibly as thin as 1 km. The imaged disk of emitting thermosphere is about 7 km in diameter. Hence, auroral structures may sometimes cause large-intensity gradients within the imaged disk and hence present a mixed polarization situation when the image is treated as a single pixel. This may be a cause of some of the disturbance in the apparent polarization measurements. The second is the fact that the observations are not made below the local point H but integrated along the line of sight to H, where the magnetic field configuration and the electron precipitations may vary. To solve this issue, measurements of the polarization from several remote locations should be carried out allowing for a 3-D reconstruction of the polarized emission. The third limitation resides in our assumption that the emission maximizes at 220 km. This is probably correct in average since the mean AoLP during quiet periods is very close to the expected theoretical value but is probably not correct when geomagnetic activity increases. This is also solar cycle dependent, owing to the change of the neutral atmosphere.

For future observations, a magnetometer should be installed directly below the observed point H. Several facilities offer such a capability, in particular, Tromsø in Norway where the EISCAT radar is installed.

There is now strong evidence that the AoLP variability is at least partly an indicator of the local magnetic field variations and partly an indicator of the pitch angle distribution of the precipitating electrons. It is therefore an important parameter for future geophysical researches. On average, during quiet periods, the AoLP is a measurement of the magnetic field configuration. This has important consequences, in particular, in planetary physics, to measure how the interplanetary magnetic field (IMF) surrounds planets such as Venus or Mars: the measurement of the atomic oxygen red line polarization in their atmospheres could provide a direct picture of the IMF.

#### Acknowledgments

The present research project has been supported by the European project Europlanet 2020 RI, grant agreement 654208, working group VA1 PSWD and by the IPEV project 1026: "Polaris 2." J. Moen was supported by the Research Council of Norway grant 230935. J. Lilénsten and M. Barthélemy thank all the friends from IPEV both in Brest and in Ny-Ålesund for their continuous support and their help during the measuring season. Plots in this article have been made with the Gildas Greg software. Magnetometer data from the Greenland Magnetometer Array (Danmarkshavn) were provided by the National Space Institute at the Technical University of Denmark (DTU Space).

#### References

- Bommier, V., S. Sahal-Brechot, J. Dubau, and M. Cornille (2011), The theoretical impact polarisation of the O I 6300 Å red line of Earth aurorae, *Ann. Geophys.*, *29*, 71–79, doi:10.5194/angeo-29-71-2011.
- Clarke, D. (2010), *Stellar Polarimetry*, Wiley, Weinheim, Germany.
- Fukushima, N., and Y. Kamide (1973), Partial ring current models for worldwide geomagnetic disturbances., *Rev. Geophys. Space Phys.*, *11*, 795–853, doi:10.1029/RG011i004p00795.
- Goldstein, D. (2003), *Polarised Light*, Marcel Dekker, New York.
- Lilénsten, J., C. Simon, M. Barthélemy, J. Moen, R. Thissen, and D. A. Lorentzen (2006), Measurement of the polarisation of the oxygen thermospheric red line: A review and a prospective in the frame of Space Weather studies, *Space Weather*, *4*, S11002, doi:10.1029/2006SW000228.
- Lilénsten, J., J. Moen, M. Barthélemy, R. Thissen, C. Simon, D. A. Lorentzen, O. Dutuit, P. O. Amblard, and F. Sigernes (2008), Polarisation in aurorae: A new dimension for space environments studies, *Geophys. Res. Lett.*, *35*, L08804, doi:10.1029/2007GL033006.
- Lilénsten, J., M. Barthélemy, P. Amblard, H. Lamy, C. Simon Wedlund, V. Bommier, J. Moen, H. Rothkaehl, J. Eymard, and J. Ribot (2013), The thermospheric auroral red line polarization: Confirmation of detection and first quantitative analysis, *J. Space Weather Space Clim.*, *3*, A01, doi:10.1051/swsc/2012023.
- Lilénsten, J., V. Bommier, M. Barthélemy, D. Bernard, H. Lamy, J. Moen, M. Johnsen, U. Løvhaug, and F. Pitout (2015), The auroral red line polarisation: Modelling and measurements, *J. Space Weather Space Clim.*, *5*, A26, doi:10.1051/swsc/2015027.
- Martinez Herrero, R., P. Mejias, and G. Piquero (2009), *Characterization of Partially Polarized Light Fields*, Springer, Berlin.
- Olsen, N., T. J. Sabaka, and L. Tøffner-Clausen (2000), Determination of the IGRF 2000 model, *Earth Planets Space*, *52*, 1175–1182, doi:10.1186/BF03352349.
- Porter, H. S., F. Varosi, and H. G. Mayr (1987), Iterative solution of the multistream electron transport equation. I—Comparison with laboratory beam injection experiments, *J. Geophys. Res.*, *92*, 5933–5959.
- Schunk, R. W., and A. F. Nagy (2004), *Ionospheres*, 570 pp., Cambridge Univ. Press., Cambridge, U. K.
- Stenflo, J. (1994), *Solar Magnetic Fields, Astrophys. and Space Sci. Lib. (ASSL)*, vol. 189, Kluwer Acad., Dordrecht, Netherlands.